JOURNAL OF Applied Polymer SCIENCE

Fabrication of Low Surface Free Energy Automotive Clear Coats: Mechanical and Surface Chemistry Studies

A. Mohammad Rabea,[1] M. Mohseni,[1] H. Yari,[1,2] B. Ramezanzadeh[1]

[1]Department of Polymer Engineering and Color Technology, Amirkabir University of Technology, Tehran, Iran

[2]Institute for Color Science and Technology, Department of Surface Coatings and Corrosion, Lavizan, Tehran, Iran

Correspondence to: M. Mohseni (E-mail: mmohseni@aut.ac.ir)

ABSTRACT: This work aims at improving the surface chemistry and the mechanical properties of a commercial acrylic–melamine clear coat using a functional siliconized additive. The resistance of films against biological degradation was then investigated using pancreatin (simulated bird droppings) and Arabic gum (simulated tree gum). Variations in the surface and bulk chemical structures, as well as the thermomechanical characteristics of the clear coats at different concentrations of the additive, were investigated by a wide range of techniques inclusive of contact angle measurement, gonio-spectrophotometery, dynamic mechanical thermal analysis (DMTA), energy-dispersive spectroscopy, atomic force microscope, optical microscope, and attenuated totalreflectance Fourier transform infrared (ATR-FTIR) spectroscopy. Negligible effect of additive on color change was revealed. It was shown that even at low loadings of additive it could migrate to the surface, producing hydrophobic films with very low surface free energies with water contact angle exceeding 100°. In addition, it was found by DMTA and ATR-FTIR studies that the functional additive was covalently attached to the acrylic–melamine chains through its hydroxyl groups. However, phase separation was observed at high concentrations of additive, leading to reduced crosslinking density. The clear coat resistance against pancreatin and Arabic gum was improved using optimum concentrations of the additive. © 2012 Wiley Periodicals, Inc. J. Appl. Polym. Sci. 128: 4067–4076, 2013

KEYWORDS: coatings; crosslinking; films; surfaces; interfaces

Received 20 June 2012; accepted 19 September 2012; published online 17 October 2012

DOI: 10.1002/app.38627

INTRODUCTION

Since the advent of base coat/clear coat automotive coating systems, their use in car industries has shown to increase very rapidly. The main reason is the superior properties of this system when compared with those of conventional ones.[1–5] However, because of their weaknesses against outdoor environments, coatings appearance and durability tend to diminish through constant use. Hence, the damages will be more visible due to the high glossy characteristic of such coatings.[6,7] A common type of failure that appeared on these coatings is biological degradation. The chemical and physical properties of coatings may be greatly influenced on such a phenomenon.[8–11] It has been shown that[10–12] because of the presence of some enzymes in naturally occurring materials, they could play a vital role to chemically degrade the coating. The results showed that[13] the effect of other natural substances such as tree gum was a severe crack formation and shrinkage of the films. It was also shown that gum could strongly attach to clear coat surface before drying process commenced. During gum drying, significant stress can be exerted to the coating layers, especially the clear coat. Therefore, it is evident that degradation is the result of attachment or penetration of these materials to the surface of films. Recently, several attempts have been made[14–16] to improve the durability and the life span of the coatings system. To achieve such goals, the surface properties of coatings have shown to be highly important. As process of attachment and penetration take place after wetting of the surface by these materials, decreasing the surface free energy of the coatings can restrict the degradation.

Different approaches have been used to improve surface properties of the coating. Using additives has been the easiest method to change the surface chemistry and the morphology of the coating without performing significant changes to the coating formulation. Most of these additives, such as polydimethyl siloxanes, are silicone based and are modified with polyether and/or fluorocarbon chains in order to enhance their performance.

Polysiloxane additives are often surface active because of their low surface energy, and therefore, they tend to migrate to the surface. While the —$(CH_3)_2SiO$— groups migrate to the surface, modified organic chains remain within the bulk of the film.

Hence, the former groups cause enhanced surface slippage and increased hardness, and the latter change the viscoelastic properties. The surface migration ability of a polysiloxane additive depends on whether it is modified by polyether and/or fluorocarbon chains and their corresponding chain lengths. The used load of each additive, as well as its compatibility with polymeric chains of the clear coat, also affects its surface migration capability.[7,17–21] However, these additives may not be suitable, as they are not able to vary surface chemistry or morphology of the coating significantly. Moreover, the weak interactions of these additives with coating matrix make them less durable against weathering condition. To solve the problem, new generations of functional siliconized additives have come into existence. These additives are able to migrate to the coating surface and participate in coating curing process to produce strong durable chemical interactions with the coating matrix. Furthermore, these additives are able to reduce surface free energy much greater than the conventional ones.[17,18]

In our previous works,[22,23] a polyurethane film was modified using a reactive silicone additive in order to enhance its resistance against graffiti. The results showed that the additive could migrate to the surface and lead to reduction in surface free energy. Accordingly, a surface with less wetting characteristic could be obtained which repelled graffiti more easily.

In a similar approach, the effect of such an additive may presumably be effective to reduce the surface free energy of a stoving acrylic–melamine clear coat. Therefore, the main objective of this work is to improve the surface chemistry and the mechanical properties of an acrylic-/melamine-based films in the presence of such additives. The surface modification was done in order to enhance the clear coat resistance against biological substances. Analytical techniques were then used to reveal the influence of the additive on the chemical, mechanical, and morphological properties of the clear coats.

EXPERIMENTAL

Sample Preparation

A multilayer automotive coating system used in this study was applied on steel metal plates in the paint workshop of an automobile manufacturer (Parskhodro Co. Iran). Steel metal plates of D7-21.2 type (1.2 mm in thickness), provided by Foolad Mobarake (Iran), were used as substrate. Then, they were treated by a conversion coating in a three-cationic phosphating bath supplied by Henkel Co. The thickness of the phosphating layer was 2–5 μm. The phosphated substrate was then coated by a cationic water-borne electrodepositing coating (ED; supplied by KCC Co. (Korea)). and cured at 150°C for 20 min. The fully cured layer of ED was 15–20 μm thick. Then, the samples were painted by a primer surfacer provided by BASF Co. (Germany) and cured at 145°C for 20 min. The dry thickness of primer layer was around 30–35 μm. In the final step of painting, a black polyester/melamine basecoats (15–20 μm thick) was applied over the primer surfacer and different clear coats supplied by BASF Co. The clear coats composition is listed in Table I. The application of basecoat and clear coat was performed in a process known as wet-on-wet. Curing was conducted at 140°C for 20 min. In addition, a blank clear coat without any silicone additive [a mixture of acrylic resin with a partially butylated melamine curing agent (70:30 w/w)] was applied on the black basecoat as a reference sample (CC.0). The samples were then left for at least 1 day in ambient temperature prior to analysis.

Table I. Formulation of Various Modified Clear Coats

Sample no.	BYK-SILCLEAN 3700 (wt %)	Polyacrylate (wt %)	Melamine (wt %)
CC.0	0.00	70.00	30.00
CC.2	3.60	71.92	24.46
CC.4	7.30	70.46	24.46
CC.6	10.91	69.00	24.46
CC.8	14.61	67.54	2.51

Biological Test

Arabic gum was procured from Merck Co. (Germany). A mixture of water and gum powder (10:1) was prepared. The mixture was kept at ambient temperature for 72 h. Arabic gum solutions were exposed to 1 cm^2 area of each film. Samples were then kept in an oven at 60°C for 72 h. Water was sprayed on the surface of the samples exposed to gum after every 3 h periodically. This was done to simulate the outdoor condition.

Appearance Analysis

Color attributes changes of coatings were determined by a Macbeth CE 741 GL gonio-spectrophotometer (Macbeth, USA). Color attributes (L $a^\star$ $b^\star$) and total color difference (ΔE) were measured using CIE 1976 formula [eq. (1)][22]:

$$\Delta E_{ab} = \sqrt{(\Delta L)^2 + (\Delta a^*)^2 + (\Delta b^*)^2}. \quad (1)$$

Here, L is lightness, and $a^\star$ and $b^\star$ are red-green and yellow-blue color coordinates, respectively. Delta (Δ) denotes the difference in corresponding parameters before and after inclusion of additive.

Surface Free Energy Calculation

Wettability of the specimens was evaluated by static contact angle measurements using a "KRUSS" G2/G40 system (Hamburg, Germany). The ASTM D-724 standard was used as a reference for the procedure of calculation. To determine surface free energy, probe test liquids (analytical grade), with different values of surface tension (γ_l), were used. Five replicates were conducted in order to ensure the statistical validity of the results. The measurement was completed after about 30 s.

The method proposed by Wu and Nancollas[24] [eqs. (2) and (3)] was used to calculate the surface free energy of the coating samples.

$$\gamma_{lv}(1+\cos\theta) = 4\left(\frac{\gamma_{sv}^p\gamma_{lv}^p}{\gamma_{sv}^p+\gamma_{lv}^p} + \frac{\gamma_{sv}^d\gamma_{lv}^d}{\gamma_{sv}^d+\gamma_{lv}^d}\right), \quad (2)$$

$$\gamma_{sv} = \gamma_{sv}^p + \gamma_{sv}^d, \quad (3)$$

where γ_{lv} is the liquid–vapor interfacial tension, and θ represents the Young's contact angle. γ_{sv}^p and γ_{sv}^d are the polar and disperse components of the surface free energy of solid,

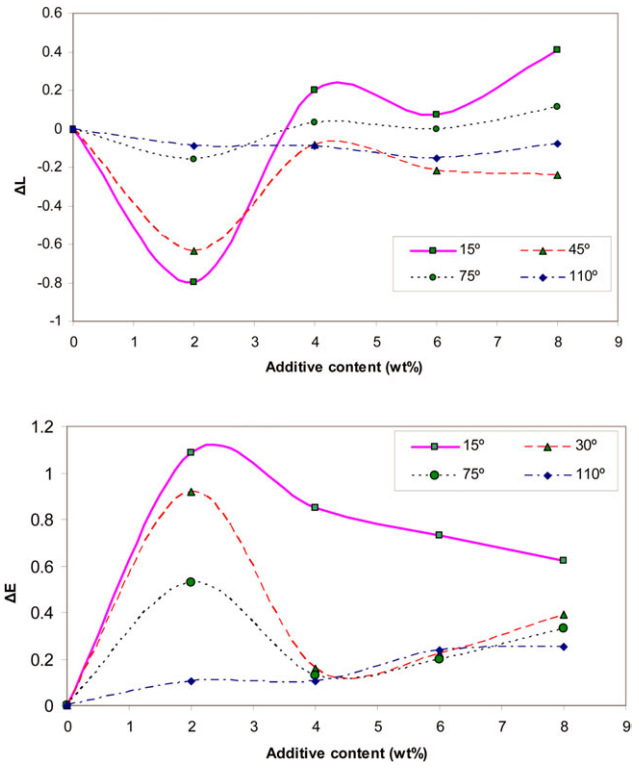

Figure 1. Variations of ΔL and ΔE versus additive content at different observation angles. [Color figure can be viewed in the online issue, which is available at wileyonlinelibrary.com.]

respectively. γ_{lv}^{p} and γ_{lv}^{d} are the polar and disperse components of surface tension of the probe liquid. γ_{sv} is the total surface free energy of the solid.

Dynamic Mechanical Thermal Analysis

Dynamic mechanical thermal analysis (DMTA) was carried out with a DMA-TRITON Model Tritec 2000 instrument (Cambridge, UK) at temperature range between −40 and 120°C and at frequency of 1 Hz. The mode of the analysis was tension, and the heating rate was 5°C/min (according to ASTM E-1640-04).

Surface Analysis

Using scanning electron microscope (Sungwoo Corp.), equipped with an energy-dispersive spectrophotometer (EDS, Cambridge, UK) analyzer, surface elemental composition of the clear coats was studied. A DME (Denmark) scanner (DS 95-50) atomic force microscope (AFM) was used to investigate the surface morphology and topography of the clear coats. The surface morphology of the samples exposed to biological materials was studied by a Leica DMR optical microscope (Germany). An attenuated total reflectance Fourier transform infrared (ATR-FTIR)spectrophotometer model Equinox X-55 (Germany) with are solution of 4 $cm^{-1}$was used to investigate the surface functional groups of the free film samples containing the silicone additive. Samples were test edin the transmissionmode.

Table III. Contact Angles (θ) of Water, Diiodomethene, and Benzyl Alcohol on the Surfaces of the Films

Sample	Water	Diiodomethene	Benzyl alcohol
CC.0	77.0	49.5	23.0
CC.2	100.8	75.5	61.8
CC.4	104.3	75.6	66.1
CC.6	104.6	75.2	66.2
CC.8	104.8	74.7	65.8

RESULTS AND DISCUSSION

Appearance Measurement

Color attributes changes of the clear coat after addition of additive were studied by a gonio-spectrophotometer. Variations of ΔL ($L_2 - L_1$) and ΔE before and after inclusion of additive were studied at four observation angles as depicted in Figure 1.

As it can be seen from Figure 1, the additive can influence the appearance parameters. An increase in ΔE and decrease in ΔL of the clear coats are more obvious at 2 wt % additive loading. The corresponding ΔL values for this sample are negative. However, at higher concentrations, the difference in lightness tends to decrease, thereby decreasing ΔE. Further addition of additive gives rise to depreciation of ΔE for the samples containing greater additive contents. Variations of ΔE and ΔL parameters are more significant at near specular angles (15° and 45°). The decrease in ΔL (negative values) and the increase in ΔE indicate that additive influences coating appearance negatively at low loadings. In fact, additive migration to the surface of the clear coat may have two different effects on the surface morphology. Additive could then act as a matting agent. This matting effect may be explained by the migration of additive to the surface. On the other hand, additive can increase clear coat surface smoothness by affecting its surface free energy. Accordingly,

Table II. Color Attributes Differences of the Clear Coats After Marker Removal as Obtained from Gonio-Spectrophotometry

			Appearance parameters					
Sample	ΔL		Δa		Δb		ΔE	
	20°	110°	20°	110°	20°	110°	20°	110°
CC.0	4.35	−1.05	−0.084	0.426	2.05	1.05	6.49	1.53
CC.2	2.54	−0.95	−0.736	0.244	0.431	0.777	3.69	1.25
CC.4	1.056	−0.84	−0.157	0.168	0.246	0.769	1.52	1.15
CC.6	0.95	−0.82	−0.216	0.075	0.563	0.669	1.47	1.06
CC.8	1.20	−0.89	−0.174	0.148	0.650	0.610	2.20	1.08

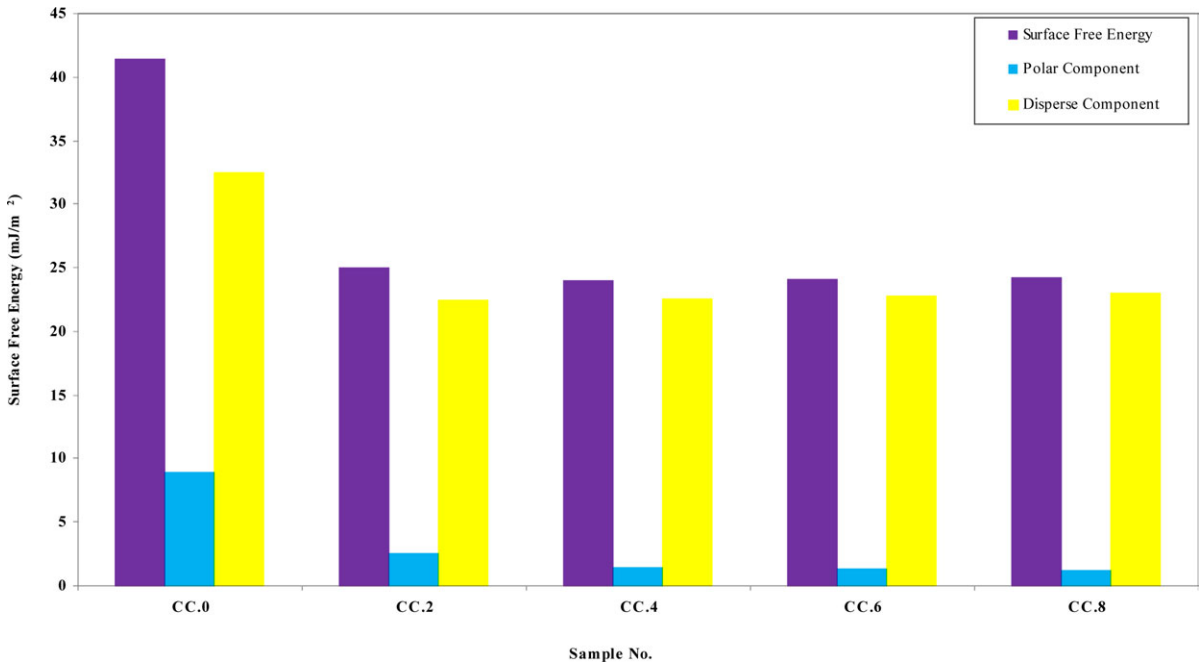

Figure 2. Surface free energy of the coating samples. [Color figure can be viewed in the online issue, which is available at wileyonlinelibrary.com.]

additive enhances the leveling, resulting in higher smoothness. It can be expected that additive migration to the clear coat surface can be responsible for the reduced ΔL and increased ΔE at low loadings. In addition, to investigate the effect of the silicone additive on cleanability of the surfaces, marker test was applied on the samples. For this purpose, first an area of 4 cm × 4 cm of the surface was colored by a black marker (Staedtler, Germany). Then, the surface was cleaned by a dry paper tissue, and the color difference before any marking and after removing the marker was investigated. Table III shows the color attributes differences of the samples. It is clear that by increasing the concentration of the additive, the color differences decrease. This is because of the migration of the silicone additive to the surface of the samples, which reduced the surface free energy and increased the cleanability of the samples. Table II shows that for CC.8, the color differences are larger than that of CC.6 because of the reduction in crosslinking density of this sample.[22] The results of DMTA can confirm this observation.

The values of contact angle of the clear coats containing different concentrations of additive are shown in Table III.

According to Table III, in the presence of silicone additive, the surface characteristic of the clear coat can be shifted from hydrophilic to hydrophobic. However, the incorporation of higher amounts of additive exceeding 4 wt % cannot affect the contact angle notably, maintaining the contact angle at about 104°.

Using the model proposed by Wu and Nancollas,[24] the values of surface free energy of the clear coats were calculated. Surface free energies of different samples are given in Figure 2.

As can be seen in Figure 2, increase in additive concentration has declined the surface free energy of the films. Results can also show negligible differences between the values of surface free energy of CC.4, CC.6, and CC.8. This may be explained by additive chains migration to the surface of the films as they have lower surface tension relative to that of the resin formulation, resulting in population of additive at the surface.[22,23] Figure 2 shows that the addition of additive to the clear coat formulation reduces both γ_{sv}^{d} (disperse component of surface free energy) and γ_{sv}^{p} (polar component of surface free energy). However, at concentrations greater than 4 wt %, the γ_{sv}^{d} and γ_{sv}^{p} are not significantly changed. It can be expected that decrease in the surface free energy may lead to poor interaction between coating and biological materials, resulting in an improvement in resistance of the sample against biological degradation.[25] The results show that the decrease in polar component is significantly greater than that of the disperse part. It is well known that additive has lower polarity when compared with acrylic/melamine matrix. Therefore, additive migration to the surface of the clear coat may seem responsible for the decrease in surface polarity and therefore γ_{sv}^{p}. On the other hand, it seems that the disperse part of the additive has higher polarity than the disperse part of the clear coat. This can be understood by the effect of additive on the decrease of γ_{sv}^{d}.

The effects of additive on the mechanical properties of the clear coat have been studied by DMTA analysis. Variations of storage modulus and tan δ versus temperature are shown in Figure 3. The values of glass transition temperature (T_g) and loss peak height are deduced from DMTA graphs (Table IV).

It can be seen that additive can improve mechanical properties of the clear coat by producing strong physical/chemical networks. The results show a higher storage modulus of the clear coat containing 4 wt % additive from −40 to 30°C when compared with the blank sample. This may be attributed to the physical chain entanglement of additive and resin chains, which prevents the movement at temperatures lower than T_g. Moreover, additive includes hydroxyl groups that could produce

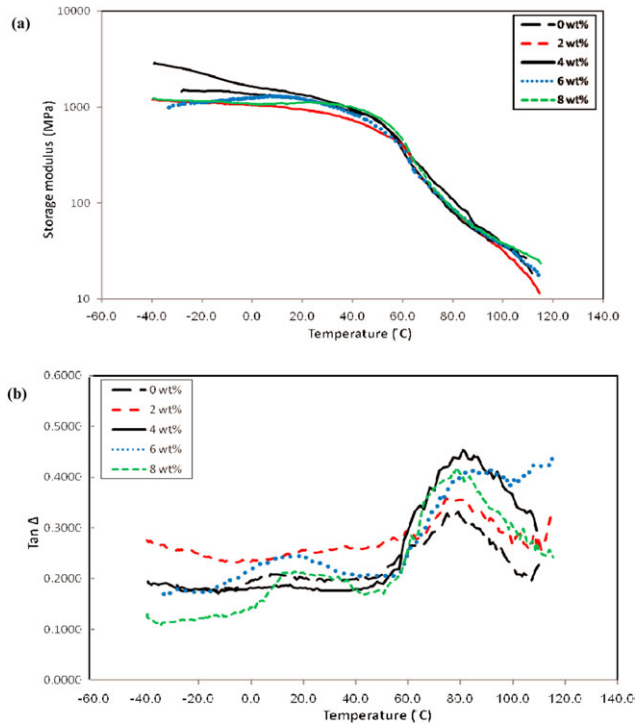

Figure 3. Storage modulus (a) and tan δ (b) versus temperature for different samples. [Color figure can be viewed in the online issue, which is available at wileyonlinelibrary.com.]

hydrogen bonds with the coating matrix, leading to the increase of the storage modulus. However, addition of higher additive contents to the clear coat formulation does not cause greater coating storage modulus. The results show negligible difference between storage modulus of the samples at glassy region. However, the storage modulus was reduced in the presence of additive at temperatures greater than 110°C (plateau rubbery zone). Although the decrease in storage modulus is not so significant, it shows that additive may involve in the curing process of the clear coat. Taking into account that O—H contents of additive and acrylic polyol are 3.6 and 4.5, respectively, the inclusion of this reactive additive will presumably result in a decrease in crosslinking density. In CC.2 and CC.4 formulations, as the concentration of additive is low, the reduction in storage modulus, because of the depreciation in crosslinking density, has less effect when compared with the increased storage modulus. This contradiction is due to the improvement in physical entanglement by adding silicone additive. This is because of formation of hydrogen bonds between the unreacted hydroxyl groups.[22] Therefore, the increase in color differences for CC.8 can be attributed to the decrease in crosslinking density of the sample resulting in increased penetration of the marker inside the sample.

Table IV. T_g and Loss Peak Height Deduced from DMTA for Different Samples

	T_g (°C)		
Sample	T_{g1}	T_{g2}	Loss peak height
CC.0	79.20	-	0.35
CC.2	79.20	-	0.35
CC.4	81.10	-	0.45
CC.6	83.30	13.60	0.40
CC.8	77.20	15.20	0.41

Table V. Proportions of Normalized Hydroxyl Group and Etheric Bond in ATR-FTIR Spectra

	Sample				
Bond	CC.0	CC.2	CC.4	CC.6	CC.8
OH/CH (3100–3600 cm^{-1})	0.221	0.232	0.248	0.259	0.268
Ether/CH (900–1100 cm^{-1})	0.826	0.837	0.804	0.682	0.665

As it can be seen in Figure 3 and Table V, the addition of additive can increase T_g (T_{g1}) of the samples. The reason might be due to the presence of physical entanglement in samples containing additive and the hydrogen bonds formed. This effect plays an important role for increasing T_g when compared with the reduced crosslinking density at lower concentrations of additive. However, for samples containing higher amounts of additive (CC.8), the decrease in T_g due to reduction in crosslinking density can be observed. The results also show that by increasing the additive concentration, the peak height and also the difference in half-width temperature of maximum tan δ have increased. This corresponds to the increase in damping and phase separation. Furthermore, tan δ versus temperature curves show that samples containing 6 and 8 wt % of silicone additive have two peaks. This phenomenon confirms the occurrence of phase separation because of the greater presence of silicone additive. This finding is in agreement with surface free energies data. Figure 2 showed that surface free energy decreased by increasing additive concentration up to 4 wt % and remained almost constant. It shows that in CC.4, there is a maximum possible amount of additive at the surface of the film. Hence, adding more additive does not have any significant effect. Therefore, extra additive remains on the bulk of the samples and, because of the difference in surface tension of additive when compared with clear coat formulation, tends to form more aggregation. This is perhaps why there are two T_gs for CC.6 and CC.8.

To confirm the results of contact angle and DMTA, elemental map analysis using EDS and ATR-FTIR analysis were done for different samples. EDS spectra of samples containing different concentration of silicone additive are shown in Figure 4.

It shows that by increasing the concentration of additive, the amount of silicone on the surface will increase. This increase is considerable from CC.0 to CC.2 samples. However, by increasing more additive, similar values are observed. In addition, there is around 0.28 wt % of silicone in CC.0 sample. This is perhaps because of the presence of siliconized-based leveling and antifoaming additives presented in the blank sample formulation. Typical Si maps, AFM micrographs, and the schematic illustration of the clear coats containing 4 and 8 wt % additive are shown in Figure 5.

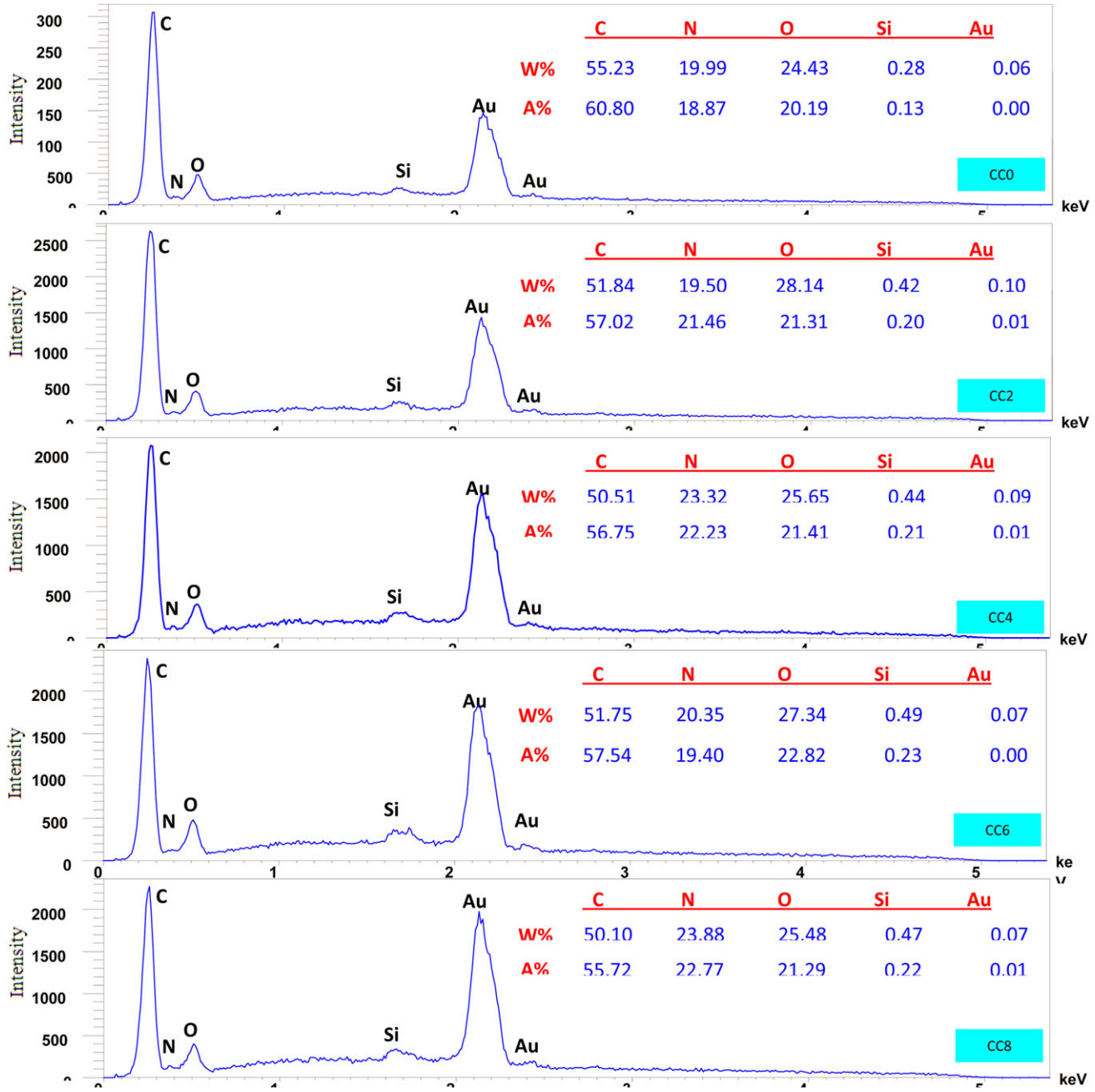

Figure 4. EDS results of various clear coats. [Color figure can be viewed in the online issue, which is available at wileyonlinelibrary.com.]

As can be seen in Figure 5, the silicon map of the clear coat containing 4 wt % additive shows a homogeneous Si distribution. This micrograph does not show any obvious phase separation. However, the Si distribution of the sample loaded with 8 wt % additive is not as homogeneous as that of the sample containing 4 wt % additive. There are areas in the EDS map of the latter sample showing Si agglomerations. This may confirm the additive chains entanglement that results in phase separation. The phase separation of the additive can also be studied by AFM analysis. As can be seen, the surface roughness of the clear coat has not significantly changed by the addition of 4 wt % additive when compared with the blank sample. On the other hand, the roughness has significantly increased using 8 wt % additive. This may be explained by the additive phase separation and chain entanglement at the clear coat surface. In fact, all of these observations show that additive compatibility with the coating matrix may depend on the additive concentration. At high additive loadings, the coating surface can be enriched of the additive. As a result, there would not be enough melamine crosslinker to react with the hydroxyl groups of the additive. This may lead to the physical interaction among the additive chains producing a new phase rich of the additive.

To investigate the surface of the samples, ATR-FTIR analysis was also done. ATR-FTIR spectra of the samples and the ratio of

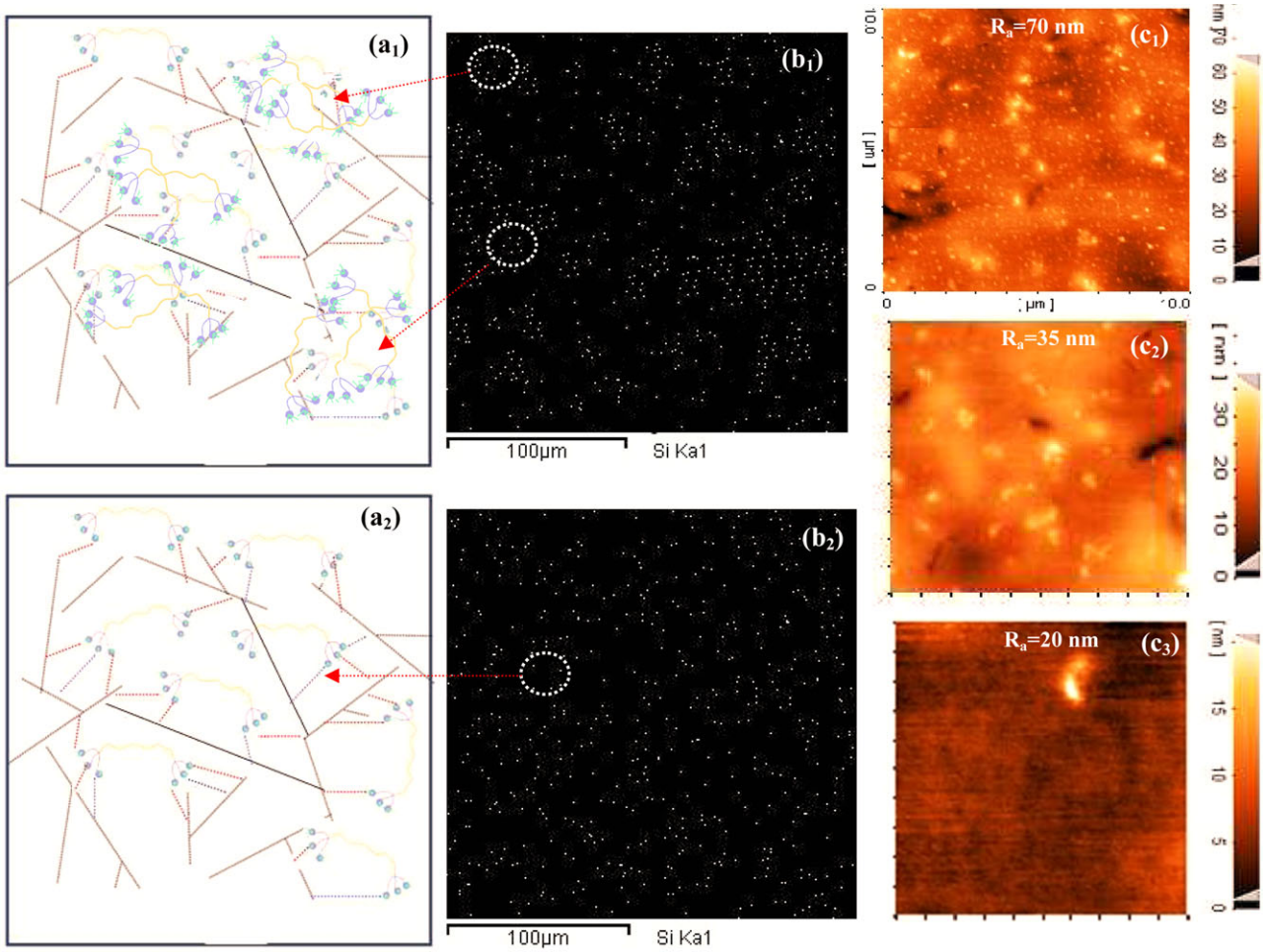

Figure 5. EDS map (b_1 and b_2), AFM micrographs (c_1, c_2, and c_3), and schematic illustrations (a_1 and a_2) of the crosslinked matrix of the clear coats containing additive (subscript 1 denotes to the clear coat containing 8 wt % additive, subscript 2 denotes to the clear coat containing 4 wt % additive, and subscript 3 refers to the blank clear coat). [Color figure can be viewed in the online issue, which is available at wileyonlinelibrary.com.]

hydroxyl group and etheric bond after normalization to the C—H vibration frequency are shown in Figure 6 and Table V, respectively.

Figure 6 and Table V show that the presence of silicone additive up to 4 wt % does not have a significant effect on the reaction of the components. It is clear that despite additive migration to

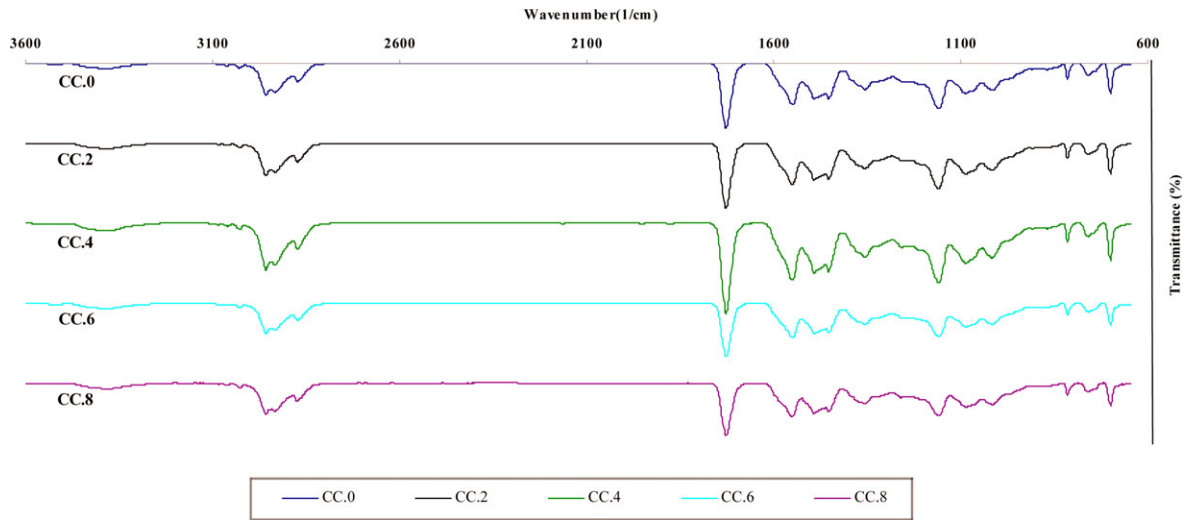

Figure 6. ATR-FTIR spectra for different samples. [Color figure can be viewed in the online issue, which is available at wileyonlinelibrary.com.]

Applied Polymer SCIENCE

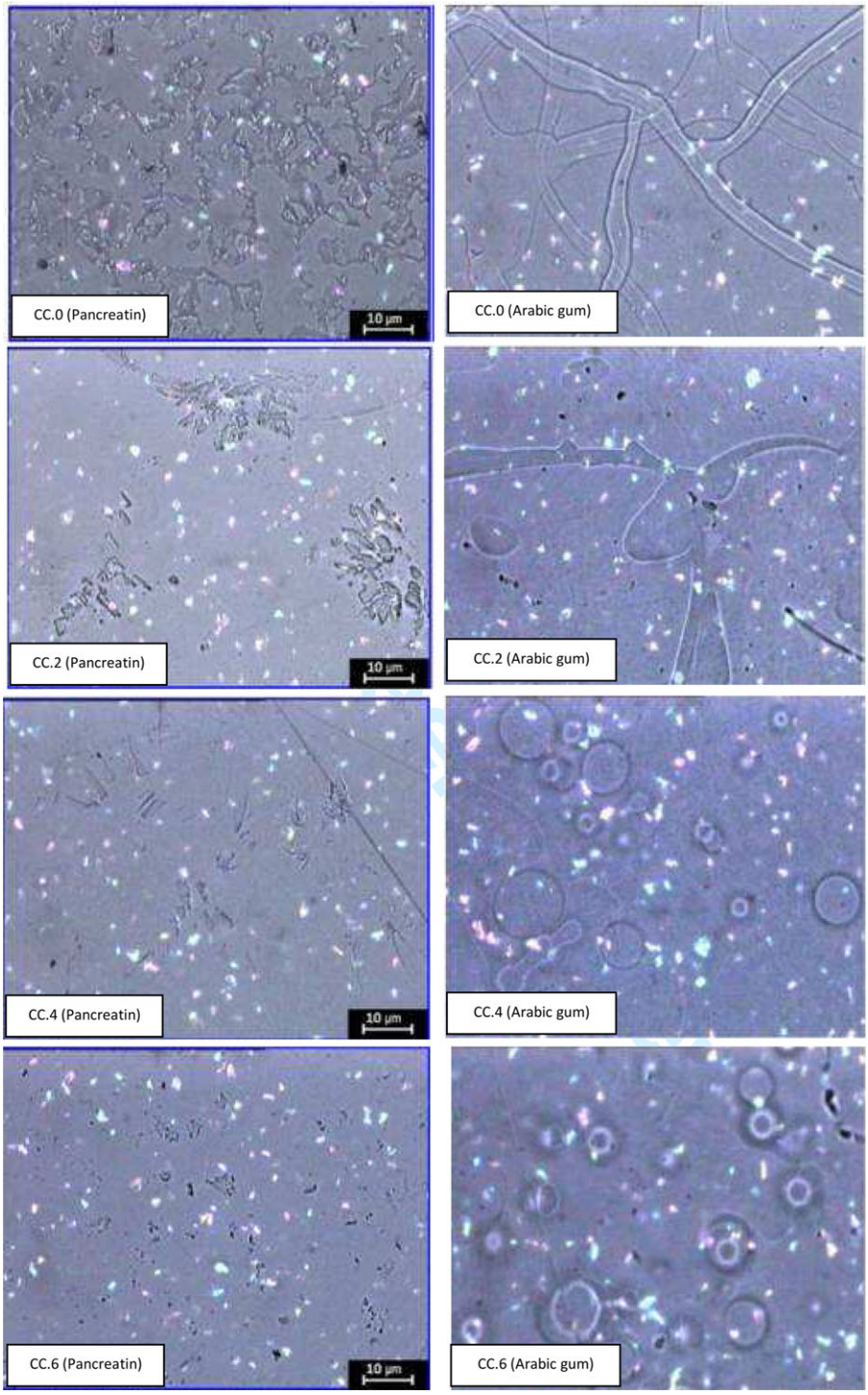

Figure 7. Optical pictures of the clear coats exposed to biological materials including pancreatin and Arabic gum. [Color figure can be viewed in the online issue, which is available at wileyonlinelibrary.com.]

the surface of the samples (increased concentration of hydroxyl groups at the top layers of the film), according to the values of the normalized hydroxyl groups and etheric bonds, this phenomenon could not significantly change the rate of reaction. However, higher concentrations of additive (CC.6 and CC.8) increased the O—H groups and decreased the etheric functionality at the surface of the samples and led to reduction in cross-linking density. It might be because of the occurrence of phase separation in these samples (based on DMTA results), which increased the hydroxyl groups in some areas and restricted the rate of reaction between O—H groups and melamine in those areas. These results are in agreement with DMTA analysis.

The increase in O—H value of the surface of the samples may contradict to the surface free energies data. The reason is that according to contact angles data, surface free energy has decreased by increasing additive concentration up to 4 wt % and remained almost constant. However, it is necessary to consider that the penetration of the ATR-FTIR analysis through the samples is in micron range and that the very top layer of the samples (in nanometer range) is responsible for surface free energy phenomenon. Therefore, it is possible that phase-separated silicone additive exposed the silicone parts to the film–air interface leaving hydroxyl groups remained on the bulk of the films thereby lowering the surface free energy. Thus, adding greater amount of additive did not change the surface free energy of the samples.

To evaluate the additive effects on the clear coats biological performance, the coatings surface morphology after biological attack are studied by an optical microscope. The biological materials that are used in this regard are simulated tree gum (Arabic gum) and simulated bird dropping (pancreatin) (Figure 7).

Figure 7 shows that pancreatin causes severe etching of the clear coat surface as a result of chemical hydrolytic degradation. On the other hand, the degradation that occurred on the clear coat surface exposed to Arabic gum was mainly in the form of crack formation indicating physical degradation. Severe crack formation and chemicals etching can be seen on the blank clear coat exposed to Arabic gum and pancreatin, respectively. The Arabic gum solution could strongly attach to the clear coat surface and perform severe stress during drying, which can overcome the clear coat cohesiveness leaving cracks on the clear coat surface. Pancreatin is also consisting of different kinds of enzymes that are responsible for the clear coat hydrolytic degradation. Using additive, both the number and the size of the cracks and etched areas have significantly changed. The number of cracks and etched areas are reduced significantly at 4 wt % additive. This observation shows that additive could improve the coating resistance against biological degradation by affecting the surface properties. It has been shown that additive could increase contact angle by reducing the surface energy. Moreover, the clear coat surface modulus was increased using 4 wt % additive. Biological materials are solved in water. The reduction of surface free energy results in a weaker interaction between the biological substances and the clear coat surface. Furthermore, they cannot penetrate into the coating matrix easily. As a result, the additive can prevent the clear coat degradation by controlling surface mechanical and chemical properties.

CONCLUSION

It was found that by adding 4 wt % of an OH-functional silicone additive into a commercial acrylic–melamine film, the surface and mechanical properties of the clear coat improved. The surface hydrophobicity tended to increase. The migration of nonpolar part of the additive was shown to be responsible for such a behavior. In addition, a physical entanglement was shown to be responsible for the improvement in physical and mechanical properties, the influence of which was enhanced modulus and T_g. However, after the addition of certain amount of additive, phase separation was probable, leading to depreciation in crosslinking density. The results showed that using certain values of the additive could significantly enhance the clear coat resistance against biological degradation.

ACKNOWLEDGMENTS

The authors express their gratitude to Dr. S. M. Mirabedini from Iran Polymer and Petrochemical Institute for his useful discussion and Mr. R. Mafi for preparation of the materials.

REFERENCES

1. Tahmassebi, N.; Moradian, S. *Polym. Degrad. Stab.* **2004**, *83*, 405.
2. Lin, L.; Blackman, G. S.; Matheson, R. R. *Prog. Org. Coat.* **2000**, *40*, 85.
3. Rey, J.; Hartman, M. In Surcar, Cannes, France, **2001**.
4. Shibato, K.; Beseche, S.; Sato, S. In Proceedings of the PRA Fourth Asia Pacific Conference on Advance in Coatings, Inks and Adhesives; Paint Research Association, International Center for Coating Technology: Hong Kong, 1994; Paper *4*:1–11.
5. Barna, E.; Bommera, B.; Kürsteinera, J.; Vitala, A.; Trzebiatowskia, O. V.; Kochb, W.; Schmidc, B.; Graule, T. *Compos. A* **2005**, *36*, 473.
6. Liu, L. M.; Qi, Z. N.; Zhu, X. G. *J. Appl. Polym. Sci.* **1999**, *71*, 1133.
7. Mohseni, M.; Ramezanzadeh, B.; Yari, H. In New Trends and Developments in Automotive Industry; Chiaberge, M.Ed.; Intech Publisher, **2011**; Chapter 16, p 267.
8. Gaszner, K.; Neher-Schmitz, H.; Kuntz, T. A report by Forschungsinstitut for Pigment and Lake eV (FPL), Global automotive manufacturing & technology, **2003**, 1–4.
9. Ramezanzadeh, B.; Mohseni, M.; Yari, H. *Prog. Org. Coat.* **2009**, *66*, 149.
10. Yari, H.; Mohseni, M.; Ramezanzadeh, B. *Prog. Org. Coat.* **2009**, *66*, 281.
11. Ramezanzadeh, B.; Mohseni, M.; Yari, H.; Sabbaghian, S. *Prog. Org. Coat.* **2009**, *66*, 149.
12. Ramezanzadeh, B.; Mohseni, M.; Yari, H.; Sabbaghian, S. *J. Therm. Anal. Calorim.* **2010**, *102*, 13.
13. Ramezanzadeh, B.; Mohseni, M.; Yari, H. *J. Polym. Environ.* **2010**, *18*, 545.
14. Tahmassebi, N.; Moradian, S.; Mirabedini, S. M. *Prog. Org. Coat.* **2005**, *54*, 384.
15. Schulz, U.; Wachtendorf, V.; Klimmasch, T.; Alers, P. *Prog. Org. Coat.* **2001**, *42*, 38.
16. Bertrand-Lambotte, P.; Loubeta, J. L.; Verpy, C.; Pavana, S. *Thin Solid Films* **2001**, 398/399, 306.
17. Ramezanzadeh, B.; Moradian, S.; Khosravi, A.; Tahmasebi, N. *Prog. Org. Coat.* **2011**, *72*, 541.
18. Ramezanzadeh, B.; Moradian, S.; Tahmasebi, N.; Khosravi, A. *Prog. Org. Coat.* **2011**, *72*, 621.
19. Bieleman, J.; Schoiz, W.; Heilen, W.; Ferner, U.; Luers, G. In Additives for Coatings; Bieleman, J., Ed.; Wiley-VCH:

Weinheim (Federal Republic of Germany), **2001**; Chapter 5, p 139.

20. Hinder, S. J.; Loweb, C.; Maxted, J. T.; Watts, J. F. *Prog. Org. Coat.* **2005**, *54*, 104.
21. Ramezanzadeh, B.; Moradian, S.; Tahmassebi, N.; Khosravi, A. The effect of different additives on scratches and mar resistance of automotive clear coats, Paper presented at the ICE Conference, Toronto, Canada, **2007**.
22. Mohammad Rabea, A.; Mohseni, M.; Mirabedini, S. M. *J. Coat. Technol. Res.* **2011**, *8*, 497.
23. Mohammad Rabea, A.; Mirabedini, S. M.; Mohseni, M. *J. Appl. Polym. Sci.* **2012**, *124*, 3082.
24. Wu, W.; Nancollas, G. *J. Colloid Interface Sci.* **1999**, *79*, 229.
25. Ramezanzadeh, B.; Mohseni, M.; Mohammad Rabea, A.; Yari, H. *Int. J. Adhes. Adhes.* **2011**, *31*, 775.